

# 100th Anniversary of Macromolecular Science Viewpoint: The Role of Hydrophobicity in Polymer Phenomena

Jeffrey C. Foster,\* Irem Akar, Marcus C. Grocott, Amanda K. Pearce, Robert T. Mathers,\* and Rachel K. O'Reilly\*



Cite This: *ACS Macro Lett.* 2020, 9, 1700–1707



Read Online

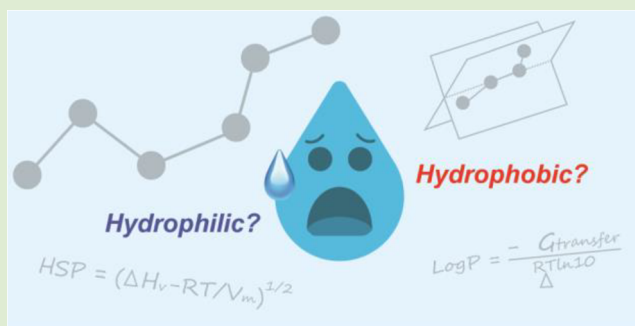
ACCESS |

Metrics & More

Article Recommendations

Supporting Information

**ABSTRACT:** The seemingly simple notion of the hydrophobic effect can be viewed from multiple angles involving theory, simulation, and experiments. This viewpoint examines five attributes of predictive models to enhance synthetic efforts as well as experimental methods to quantify hydrophobicity. In addition, we compare existing predictive models against experimental data for polymer surface tension, lower critical solution temperature, solution self-assembly morphology, and degradation behavior. Key conclusions suggest that both the Hildebrand solubility parameters (HSPs) and surface area-normalized Log  $P$  (Log  $P$  SA<sup>-1</sup>) values provide unique and complementary insights into polymer phenomena. In particular, HSPs appear to better describe bulk polymer phenomena for thermoplastics such as surface tension, while Log  $P$  SA<sup>-1</sup> values are well-suited for describing and predicting the behavior of polymers in solution.



The study of polymer structure–property relationships has fostered a deep understanding of the behavior of polymers in bulk or solution, explained phenomenological observations, inspired new research avenues in polymer synthesis and self-assembly, and ultimately facilitated the creation of novel materials. In the past few decades, many synthetic efforts have been directed toward understanding the relationships between molecular weight (MW) or molecular weight distribution (MWD) and polymer behaviors such as mechanical properties, solubility, stimuli-responsiveness, self-assembly, degradation behavior, or biological activity.<sup>1,2</sup> Such relationships invoke arguments of viscosity and chain entanglement to explain MW-dependent phenomena.<sup>3</sup> While these relationships have proven to be generally useful for a variety of polymers, they tend to exclude information regarding polymer chemistry (i.e., the specific chemical composition of the repeating unit(s)). As such, opportunities exist to connect polymer chemistry to properties, filling gaps in existing models and providing predictive information to guide future polymer design.

In pursuit of a polymer parameter to apprehend structure–property relationships, we invoke the concept of hydrophobicity. The term “hydrophobic” dates back over 100 years and has appeared in over 190k journal articles. Since many processes involve water, it is no surprise that the term “hydrophobic” is found throughout many scientific disciplines such as biochemistry, chemistry, physics, and materials science. Despite widespread qualitative use and implication in protein folding, thermal transitions, and self-assembly, predictive

models of these phenomena often struggle to quantify the influence of hydrophobicity.

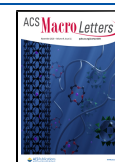
Why is it so challenging to capture hydrophobicity? Although Hildebrand and Hansen solubility parameters and partition coefficients (Log  $P$  values) have been successfully exploited to predict solution behavior of small molecules, it is a complicated transition from small molecules, many of which have rigid polycyclic structures, to large flexible macromolecules.<sup>4</sup> However, despite their limitations, studies have shown that these parameters have promise for solving scientific challenges.<sup>5–10</sup>

In this Viewpoint, we aim to examine definitions of polymer hydrophobicity and highlight important features of predictive models. Using this insight, we prioritize key parameters to compare the relative hydrophobicities of different polymers and construct structure–property relationships. We then explore the influence of hydrophobicity on polymer solution behavior and, in particular, its role in (1) polymer surface energy; (2) polymer thermal transitions (e.g., lower critical solution temperatures); (3) block copolymer self-assembly; and (4) polymer degradation via hydrolysis. We hypothesize

Received: September 7, 2020

Accepted: October 21, 2020

Published: November 4, 2020



that methods to quantify hydrophobicity which involve a combination of theory and simulations with experimental validation may provide the most robust approach. Through these explorations, the importance of considering polymer hydrophobicity in the design of polymeric materials will emerge.

## DEFINING HYDROPHOBICITY

Pure H<sub>2</sub>O possesses strong cohesive forces; thus, the act of dissolution encompasses the energetic costs of disrupting these interactions and the subsequent formation of new ones. These energetic factors strongly influence the behavior of the solute molecules, as best exemplified by the so-called “hydrophobic effect”. Familiar outcomes include “the disaffinity of oil for water”<sup>11</sup> or “the tendency for oil and water to segregate”.<sup>12</sup> The term hydrophobicity has also been used broadly in reference to polymer solubility, partitioning behavior, and aggregation, or to describe fundamental chemical properties such as polarity, although the latter is imprecise.

To expand the physicochemical basis that lies beneath, we must consider what makes a polymer “hydrophobic”. The following contributing factors reinforce the complexity of a seemingly simple idea. For instance, “hydrophobic interactions depend on the temperature, pressure, solute size and shape, type, and concentration of the additives, as well as the proximity to interfaces”.<sup>13</sup> From another angle, researchers emphasize “hydrophobicity depends not only on the surface area of a solute but also on its shape and curvature”.<sup>14</sup> These observations suggest that molecular dynamics simulations have a key role to play in obtaining information about solute surface area and curvature and that simple theoretical constructions of hydrophobicity, involving carbon counting or considering the ratio of carbon/oxygen atoms within a molecule, are insufficient. Indeed, poly(ethylene glycol) (PEG; C/O = 2) displays water solubility while poly(oxymethylene) (POM; C/O = 1) does not.<sup>15</sup>

## BRIEF TIMELINE

For small molecules and macromolecules, the avenues for quantifying hydrophobicity fall into four general categories: theory, empirical, simulations, and experimental. In the 1930s, Hildebrand pioneered a theory-based approach for predicting the solubility of small molecules by combining enthalpy ( $\Delta H$ ) and molar volume ( $V_m$ ) to give the Hildebrand solubility parameter ( $\delta$ ; eq 1).

$$\delta = \sqrt{\frac{\Delta H_v - RT}{V_m}} \quad (1)$$

Although  $\delta$  values helped to explain the swelling of vulcanized rubber,<sup>16</sup> they struggled to account for the influence of polar functional groups. Later, during the 1960s, Hansen modified Hildebrand's solubility parameter (HSP) to obtain an empirical relationship that accounted for dispersion ( $\delta_d$ ), polar ( $\delta_p$ ), and hydrogen bonding ( $\delta_h$ ) interactions between the solute and solvent molecules. In contrast, during the 1980s and 1990s, medicinal and pharmaceutical chemists gravitated toward a free-energy approach using octanol–water partition coefficients (Log  $P$ ; eq 2).<sup>17,18</sup> *n*-Octanol was chosen to mimic lipid-like structures ubiquitous in nature. By the late 1990s, sophisticated cheminformatics approaches to calculating Log  $P$  values emerged that encompassed atom-based, group-based, and mixed atom/group methods.<sup>19</sup> In contrast to other

models, the sign of Log  $P$  values (eq 3) provides a convenient indication of hydrophobicity and hydrophilicity, as insoluble or soluble compounds possess positive or negative Log  $P$ , respectively.

$$\text{Log } P = \frac{-\Delta G_{\text{transfer}}}{RT \ln 10} \quad (2)$$

$$\text{Log } P = \text{Log} \left( \frac{[\text{solute}_{\text{octanol}}]}{[\text{solute}_{\text{water}}]} \right) \quad (3)$$

In 1999, seminal work by Lum, Chandler and Weeks (LCW) was developed that acknowledged the important relationship between hydrophobicity and length scale.<sup>20</sup> This idea provided a missing piece for many hydrophobicity models: at small length scales, hydrophobicity scales linearly with molecular volume while at large length scales the situation changes and hydrophobicity scales with surface area.<sup>12</sup> Typically, the crossover from small to large length scales occurs at about 1 nm.<sup>21,22</sup> Moreover, throughout the last two decades, widespread agreement on the concept of a crossover has emerged from theory, experiments, and simulations.<sup>23–25</sup>

## COMPONENTS OF A HYDROPHOBICITY MODEL

Importantly, the concept of hydrophobicity could refer to a molecular average or to specific regions of a molecule. For instance, a polymer comprised of both a hydrophobic backbone and hydrophilic side chains may possess an overall degree of hydrophobicity that allows dissolution in H<sub>2</sub>O. Alternatively, a hydrophobic initiator might be employed in the synthesis of a hydrophilic polymer to yield a macromolecule that is water-insoluble. In addition to these examples, variation in polymer architecture must also be considered. As such, a robust hydrophobicity model should accommodate a range of possibilities. In order to understand which attributes of a hydrophobicity model would allow the most versatility, we highlight five components.

First, representations of the polymeric microstructure with a molecular model should be informed by experimental data to adequately account for the influences of composition, branching, cross-linking, and stereochemistry.

Second, a molecular model should be large enough (in terms of repeat units) to represent a polymer chain, but small enough to allow reasonable computation times. As suggested by LCW theory, the hydrophobicity of polymers below a critical length scales with their volumes and above with their surface areas. Thus, an accurate model should include the appropriate structural parameter. Indeed, some authors argue that determining length scale crossover “must be a central requirement of any comprehensive theory of the hydrophobic effect”.<sup>23</sup> As a caveat, while 5–10 monomer units exceeds the crossover length for linear polymers,<sup>26</sup> additional units may be needed to account for comonomers or branching.<sup>27</sup>

Third, our view is that a robust model must include a thermodynamic parameter. Addressing hydrophobicity from a thermodynamic perspective not only enables rigorous quantification, but also provides a theoretical basis for prediction. Both the HSP, which includes the heat of vaporization of the solvent ( $\Delta H_v$ ), and Log  $P$ , which is related to the free energy of transferring a solute molecule between phases, represent potentially useful descriptors of hydrophobicity on the basis of this view.

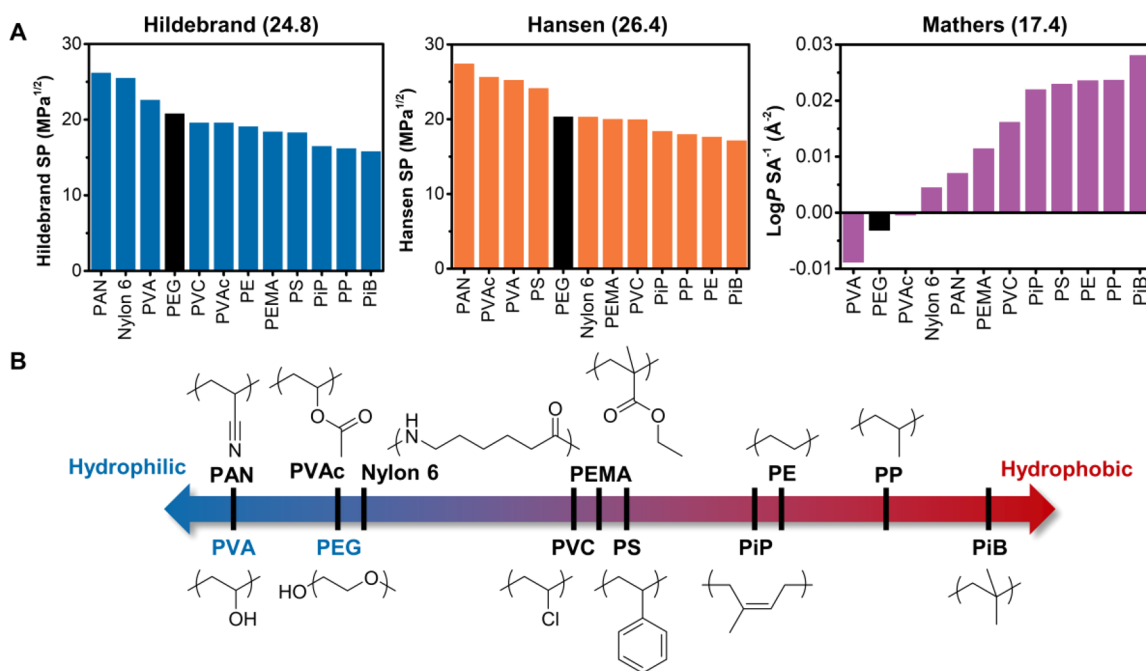


**Figure 1.** (A) Polymer hydrophobicity as ranked by the HSP, Hansen, and MHP models. In each case, hydrophobicity increases from left to right. The number in parentheses represents the least-squares error for each of these rankings compared with the average ranking shown in B. (B) Schematic representation of the average hydrophobicity ranking of each polymer, generated from the data in A.

Fourth, a structural parameter is needed to complement thermodynamic descriptors and account for molecular size. Ideally, a structural parameter would be measured after an MD simulation. Fortunately, over the last several decades, many researchers have laid the foundation for methods to calculate the surface area of macromolecules.<sup>28,29</sup> In view of LCW theory, we hypothesize that surface area (SA) is more appropriate for macromolecules than volume.

Fifth, since “hydrophobic interactions increase in strength with increasing temperature”, models should have some ability to capture the role of temperature.<sup>12</sup> As shown in eqs 1 and 2, both HSP and Log *P* have temperature dependence, while the Hansen model lacks a temperature term.

## EVALUATING PREDICTIVE MODELS

In the context of polymers, promising hydrophobicity descriptors normalize thermodynamic parameters by structural parameters, as demonstrated by HSP and, more recently, by Log *P* SA<sup>-1</sup> values,<sup>27</sup> which we term the Mathers hydrophobicity parameter (MHP). We will also consider Hansen solubility values for common polymers. In the subsequent sections, we will compare common hydrophobicity descriptors, including HSP, Hansen solubility parameters, and MHP values, against experimental data for polymers, with the aim of addressing their usefulness in constructing future predictive models.

As mentioned above, the HSP, Hansen, and MHP models of hydrophobicity have all been exploited to explain polymer behavior. Since each approach differs in the way hydrophobicity is quantified, the following question arises: which method(s) provides representation for the widest range of functional groups and polymer architectures? Beyond this, can one single method be used to explain a broad variety of experimental observations such as LCST or self-assembly behavior? Figure 1A shows a hydrophobicity ranking for 12 common polymers using the three approaches. These data can

then be used to determine an average hydrophobicity ranking by comparing the rankings of the individual methods (Figure 1B). The trends emergent in Figure 1 are generally constant with expectations. PVA, a water-soluble polymer, is on average the most hydrophilic, while those polymers comprised of exclusively hydrocarbon constituents (e.g., PP) are most hydrophobic. It should be noted that both the HSP and Hansen models ranked PAN (water insoluble) more hydrophilic than PEG (water-soluble) and PVC more hydrophilic than the ester-containing PEMA. Thus, from an observational perspective, the MHP appears to better reflect the realities of polymer water solubility. When comparing the methods quantitatively, MHP values appear to best represent the average of the three (as judged by its low LSE value). Although Hansen parameters have achieved a moderate level of success, the empirical nature of this model lacks a thermodynamic component, length scale, and adjustment for temperature. Consequently, while Hansen parameters are conceptually valid, we exclude this model from further consideration. These findings are supported by a more expansive comparison of the HSP and Hansen models, which showed they had similar prediction accuracies for polymer solvents and nonsolvents, but that neither model captured the influences of temperature, concentration, or polymer molecular weight.<sup>4</sup> To better understand the usefulness of the HSP and MHP models in a practical context, we will compare them against experimental data in the subsequent sections.

## HYDROPHOBICITY AND POLYMER PHENOMENA

**Polymer Surface Energy.** Surface tension data has been extensively used to approximate the hydrophobicity of polymers;<sup>30–32</sup> however, modern computational methods have not been rigorously tested against experimental data. To this end, we sought to investigate the relationship between the surface tension of solid polymers and MHPs/HSPs. Surface tension and polymer solubility are interrelated via



intermolecular forces, as described by the concept of cohesive energy density. Building upon Hildebrand's work for estimating polymer solubility, eq 5 was proposed for estimating polymer surface tension,  $\gamma_l$ , from cohesive energy density,  $e_{\text{coh}}$ .<sup>33</sup>

$$\gamma_l \approx Ae_{\text{coh}} \cdot V_m^{1/3} \quad (5)$$

It is, however, important to recognize that the trends in water solubility are not always replicated in terms of surface tension. For example, PVA and PEG are both water-soluble, hydrophilic polymers; however, PVA, by comparison, has notably lower surface tension (Figure 2B).

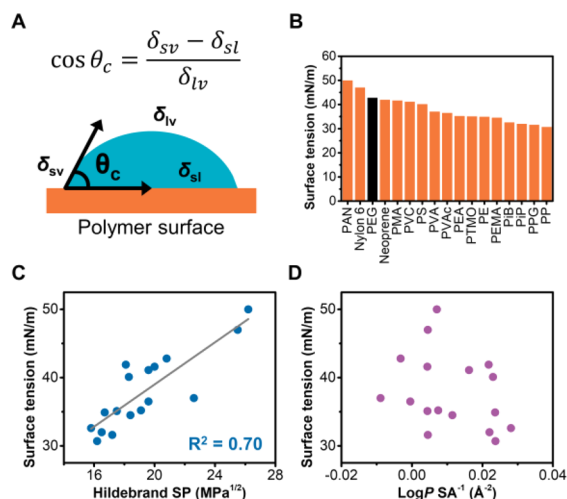


**Figure 2.** (A) Method for determining polymer surface tension using contact angle measurements. (B) Selected polymers ranked by their surface tensions. (C) Plot of surface tension vs HSP. The gray line represents a linear fit of the data with  $R^2 = 0.70$ . (D) Plot of surface tension vs MHP.

Because the process of wetting a polymer surface involves both the creation of a new interface as well as the disruption of intermolecular interactions between H<sub>2</sub>O molecules, we anticipated observing a correlation between HSPs and polymer surface tension values. Indeed, linear regression analysis revealed that the HSP model adequately described the surface tension data (Figure 2C) for linear homopolymers.

In contrast, there was no apparent linear relationship between  $\text{Log } P \text{ SA}^{-1}$  and polymer surface tension (Figure 2D). Since  $\text{Log } P \text{ SA}^{-1}$  does not directly acknowledge the intermolecular forces that govern surface tension, such as cohesive energy and internal pressure,<sup>4</sup> this result was not particularly surprising. This finding suggests that the HSP model is better suited for estimating the surface tension of water-insoluble, hydrophobic polymers. However, MHP values correlate reasonably well to water contact angles.<sup>27</sup>

**Lower Critical Solution Temperature (LCST).** Polymers that respond to temperature variations in solution display two distinct behaviors known as the upper critical solution temperature (UCST) and lower critical solution temperature (LCST). UCST and LCST are the temperature points above or below which polymers are completely miscible with the solvent.<sup>34</sup> Such transitions occur primarily in response to the increased contribution of  $\Delta S$  to the Gibbs free energy of the system ( $\Delta G = \Delta H - T\Delta S$ ) that occurs with increasing temperature.<sup>35,36</sup> When the temperature increases: (1)

intermolecular hydrogen bonding between H<sub>2</sub>O molecules and the polymer chains are weakened; and (2) the energetic influence of water organization becomes more significant, leading to the collapse and aggregation of the polymer chains. The temperature at which a clear polymer solution undergoes a LCST and becomes cloudy is known as cloud point temperature,  $T_{\text{CP}}$ .<sup>37</sup>  $T_{\text{CP}}$  will be used as a metric of comparison for hydrophobicity below. It is generally understood that the  $T_{\text{CP}}$  is inversely related to polymer hydrophobicity, and many studies have leveraged this relationship to design stimuli-responsive copolymers with bespoke thermal transition temperatures.<sup>36,38–43</sup>

In a recent work by our groups, the  $T_{\text{CP}}$ s of copolymers based on hydrophilic oligoethylene glycol monomethyl ether methacrylate (OEGMA) and different hydrophobic methacrylate comonomers were measured to investigate the influence of hydrophobicity on LCSTs. Although  $T_{\text{CP}}$  values correlated with MHPs for each of the various copolymers, a series of parallel trends for OEGMA with methyl, ethyl, butyl, and hexyl methacrylates indicated bottlebrush-like copolymers demonstrated solution behavior that was difficult to predict with oligomeric models.<sup>9</sup> Thus, we attributed these challenges to the overriding influence of side chain (grafting) density. This was surprising, since some precedent existed for using the MHP method for branching due to multifunctional monomers,<sup>27</sup> lightly cross-linked films,<sup>26</sup> and cross-linking that resulted from post-polymerization modification.<sup>44</sup> Based on these observations, we wondered the following: does hydrophobicity more directly influence  $T_{\text{CP}}$  trends for linear polymers?

Toward this end, we compared HSPs and MHPs to experimental  $T_{\text{CP}}$  values for homopolymers (from the literature). As shown in Figure 3A, no relationship was observed between HSP and  $T_{\text{CP}}$ . In contrast, two clusters of data points were evident in the plot of  $T_{\text{CP}}$  vs MHP, both of which appeared to contain data for which linear correlations could be drawn (Figure 3B). Indeed, model-based clustering algorithms identified these two clusters as statistically significant.

Based on the theoretical basis for the HSP, it is apparent that the LCST does not significantly influence the overall cohesive energy density of the solvent, at least under the dilute conditions that are typically employed during  $T_{\text{CP}}$  measurements (ca. 1–5 mg mL<sup>-1</sup> polymer). It is also apparent that the molar volume component of the Hildebrand model is insufficient to capture the chain collapse/phase separation events that occur during the LCST. Thus, the absence of a relationship in Figure 3A can be explained on these bases. Critically, the MHP appears to better describe the LCST phenomenon as it accounts for both of the following: (1) the act of transferring polymer chains from liquid to polymer phases; and (2) the creation of a new H<sub>2</sub>O–polymer interface between these phases, both of which are understood to be important for the LCST.

Of further interest, the discrete clusters of data observed in Figure 3B correspond to polymers possessing side chains in which heteroatoms are either present or absent. Indeed, a clear step-change in  $\text{Log } P \text{ SA}^{-1}$  can be observed for these two groups in the plot of their relative hydrophobicity rankings (Figure 3C). While the slopes between  $T_{\text{CP}}$  and  $\text{Log } P \text{ SA}^{-1}$  in these two clusters appear to be similar, their  $x$ - and  $y$ -intercepts are shifted. It is unclear as to the exact physical basis for this observation; however, it may be the case that differences in

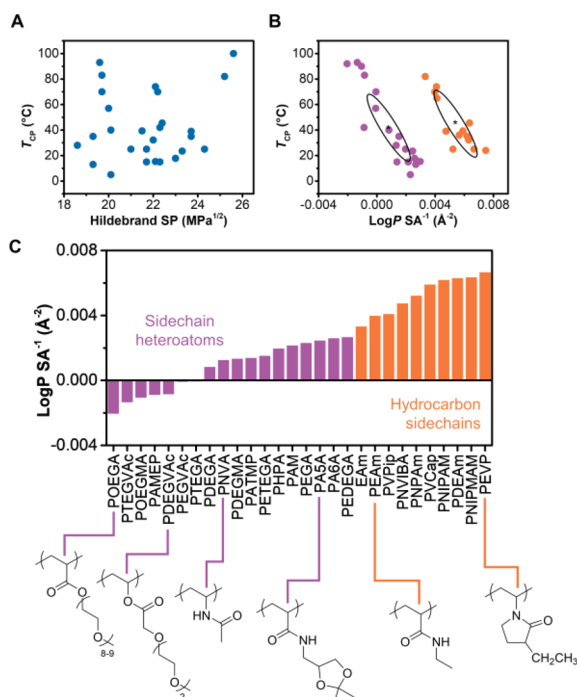


**Figure 3.** (A) Cloud point temperatures for selected polymers vs their HSPs. (B)  $T_{CP}$  as a function of MHP. Two distinct populations were identified using a model-based clustering algorithm (ellipsoidal covariance with equal volume, shape, and orientation). (C) Selected polymers with LCST behavior ranked by their MHPs. The bar colors correspond to the colors of the clusters identified in (B).

LCST mechanism exist for polymers with hydrophilic or hydrophobic side chains. This phenomenon bears further investigation.

**Block Copolymer Self-Assembly.** In aqueous solution, amphiphilic block copolymers spontaneously aggregate to form organized structures. This process, known as self-assembly, is driven by the hydrophobic effect.<sup>45–47</sup> To minimize the creation of a new interface, the hydrophobic, or core-forming, blocks of amphiphilic block copolymers aggregate to form discrete, phase-separated domains stabilized by the associated hydrophilic polymer segments. As with block copolymer self-assembly in bulk, the shapes adopted by these aggregates are related to the geometry of the constituent polymer amphiphiles.<sup>45</sup> The principal empirical relationship between amphiphile geometry and morphology is the packing parameter, which describes their packing within polymer aggregates. The packing parameter is useful for morphological prediction in systems under equilibrium; however, it does not account for the kinetic and thermodynamic factors that underlie the process of self-assembly.<sup>48–50</sup>

For flexible polymer chains, the thermodynamics of self-assembly are dominated by interfacial energy.<sup>51,52</sup> Put simply, the higher the difference in surface energies between  $H_2O$  and the polymer solutes, the higher the cost of creating a new interface during self-assembly. The simplest way block copolymers minimize energy is to simultaneously reduce the overall number of aggregates while increasing their size. However, to fill the increasing volume of these larger aggregates, hydrophilic domains must be inserted into the bulk polymer phase at additional thermodynamic cost. Thus, a tentative balance is struck between the polymer– $H_2O$  interface and the polymer–polymer interface, often resulting in the

transformation of these aggregates away from spherical morphologies toward those comprised of polymer bilayers (i.e., polymeric vesicles).

Under equilibrium conditions, the following trends in block copolymer self-assembly are anticipated: (1) morphology “increases” toward higher-order structures with increasing length of the core-forming block<sup>53</sup> and (2) morphology “increases” with increasing core-block hydrophobicity.<sup>5</sup> The former is captured by the packing parameter concept and has been well-studied in the literature. In contrast, less is known with respect to the influence of core-block hydrophobicity on self-assembly morphology.

Our groups recently reported a method to identify chemistries compatible with polymerization-induced self-assembly (PISA), a method of conducting polymer amphiphile synthesis and self-assembly simultaneously in the same pot.<sup>54–58</sup> During PISA, a hydrophilic macroinitiator (or macro-chain transfer agent) is chain-extended with a monomer that is (generally) miscible with  $H_2O$  but produces a water-insoluble polymer upon polymerization. A significant challenge of PISA is identifying monomers that fulfill the condition of solubility but produce insoluble polymers. Using *in silico* methodology, we found that such monomers could be predicted via their oligomeric  $\text{Log } P \text{ SA}^{-1}$  values, facilitating PISA formulation design.<sup>5</sup> We also showed that both nanoparticle nucleation and morphology were also well-described by  $\text{Log } P \text{ SA}^{-1}$ , directly relating a computational measure of polymer hydrophobicity to experimental observations.<sup>6</sup>

Typically, the morphologies obtained during PISA are classified according to formulation parameters using a phase diagram. Traditional phase diagrams are constructed using polymer concentration and core-block degree of polymerization (DP) as parameters. An alternative approach is to evaluate morphology based on core-block DP and hydrophobicity. Figure 4 shows phase diagrams for PISA formulations conducted using reversible addition–fragmentation chain-transfer (RAFT) polymerization plotted as a function of both DP and HSP or MHP. Note that morphologies represent a simple linear ranking, with larger “bubbles” corresponding to higher-order morphologies.

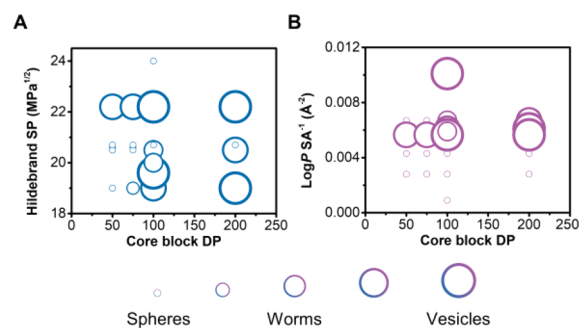


**Figure 4.** Morphological phase diagrams for self-assembled block copolymers constructed using core-forming block DP values, HSP (A) or MHP (B), and morphology. To represent morphology graphically, a ranking system was developed in which spheres, worms, vesicles, or mixed morphologies (i.e., S+W or W+V) were assigned a numerical value increasing from 1 for pure spheres up to 5 for pure vesicles. The diameters of the “bubbles” shown in A and B are proportional to these morphology rankings.

If the criteria outlined above are correct, morphology “rank” should increase as a function of both core-block DP and hydrophobicity; thus, “bubbles” corresponding to vesicles would be expected in the upper right quadrant of the phase diagram. Both HSP and MHP appear to partially capture these trends (Figure 4); however, outliers are in evidence for both treatments (these could be out-of-equilibrium morphologies). It is noteworthy that the phase diagram built with MHP appears to better represent expectations; morphologies of lower “rank” are generally located in the lower left quadrant and those of higher “rank” are located in the upper right. The superior performance of this hydrophobicity quantifier relative to HSP is hardly surprising. Recall that  $\text{Log } P$  is proportional to the free energy of transferring a molecule between organic and aqueous phases (eq 2). This type of phase transfer is integral to self-assembly; thus, the thermodynamic factors (i.e., interfacial energy) underlying the formation of block copolymer aggregates in aqueous solution are better captured by the MHP.

**Polymer Degradation by Hydrolysis.** Polymer degradation can occur by several different mechanisms depending on exposure to environmental factors such as light, heat, chemicals, or mechanical force.<sup>59,60</sup> Here, we focus on the factors that influence hydrolytic degradation, which occurs via random scission of chemical bonds in the polymer backbone to form oligomers and, eventually, monomers.<sup>61</sup> The primary underlying factor in determining the rate of hydrolytic degradation is the reactivity and electronic stability of hydrolytically labile bonds in the polymer backbone. Secondary to polymer chemistry, incorporation of comonomers to raise the glass transition temperature ( $T_g$ ) of the polymer or by the introduction of monomers to introduce crystallinity are both effective means of reducing the mobility of polymer chains and, thus, the ability of water to diffuse through the polymer network to perform hydrolytic cleavage.<sup>62,63</sup>

Likewise, enhancing polymer hydrophobicity offers an approach to reducing exposure of scissible bonds to water and has proven to be an effective means for controlling the degradation rates of polyesters.<sup>64–67</sup> Hydrophobic polymers exhibit limited bulk permeability, and slower diffusion of water into the polymer network relative to bond hydrolysis. Indeed, a recent computational study by Mathers and colleagues revealed that the propensity for hydrolytic degradation of polymers, such as polyesters and nylons, could be correlated to their hydrophobicity.<sup>68</sup>

To compare the HSP and MHP models in the context of hydrolytic degradation, bubble plots were constructed using polymer  $T_g$  and HSP or MHP values. Here, bubble size corresponds to relative degradation rates for films of selected polymers in ocean water, with the largest bubbles representing fast degradation. For polymers that degrade via hydrolysis, we expected degradation rate to be related to both hydrophobicity and  $T_g$ ; water diffusion occurs more rapidly into hydrophilic polymer films with low  $T_g$ , and thus, large bubbles should appear in the lower left quadrant of the hydrophobicity versus  $T_g$  plot. As shown in Figure 5, large bubbles tended to occupy the lower left region. From visual inspection, this trend was apparently better captured by the MHP model. We attribute outliers in both plots to polymers that are (1) highly crystalline with  $T_m$  above the temperature of the degradation experiment and/or (2) do not possess hydrolytically degradable bonds.

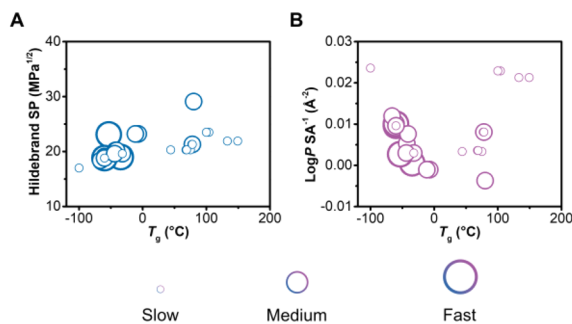


**Figure 5.** Graphical representation of bulk polymer hydrolytic degradation trends constructed using glass transition temperatures ( $T_g$ ), HSP (A) or MHP (B) values, and relative bulk polymer degradation rates. The diameters of the “bubbles” shown in A and B are literature values that reflect surface erosion data.

The use of *in silico* models to predict degradation mechanisms and quantify structure–property relationships for polymer hydrolytic degradation provides a powerful tool to inform the design of degradable materials.

## CONCLUSIONS

The concept of hydrophobicity has been implicated in a broad variety of polymer phenomena. In this Viewpoint, we aimed to better define hydrophobicity and have identified a set of five essential criteria for predictive models. Both HSP and MHP have potential to satisfy these criteria. While neither model succeeds at describing all aspects of polymer behavior, both were shown to provide value for explaining and predicting polymer phenomena such as surface energy/wetting, solution transitions, self-assembly, and degradation. When combined with experimental data, theoretical models such as the HSP and MHP represent powerful tools to aid in the design of functional, responsive materials.

## ASSOCIATED CONTENT

### Supporting Information

The Supporting Information is available free of charge at <https://pubs.acs.org/doi/10.1021/acsmacrolett.0c00645>.

Data analysis procedures, abbreviations, and data sources (XLSX)

Data analysis procedures, abbreviations, and data sources (XLSX)

Data analysis procedures, abbreviations, and data sources (XLSX)

Data analysis procedures, abbreviations, and data sources (XLSX)

## AUTHOR INFORMATION

### Corresponding Authors

Jeffrey C. Foster – School of Chemistry, University of Birmingham, Edgbaston, Birmingham B15 2TT, United Kingdom; [orcid.org/0000-0002-9097-8680](https://orcid.org/0000-0002-9097-8680); Email: [J.C.Foster@bham.ac.uk](mailto:J.C.Foster@bham.ac.uk)

Robert T. Mathers – Department of Chemistry, Pennsylvania State University, New Kensington, Pennsylvania 15068, United States; [orcid.org/0000-0002-0503-4571](https://orcid.org/0000-0002-0503-4571); Email: [rtm11@psu.edu](mailto:rtm11@psu.edu)

Rachel K. O’Reilly – School of Chemistry, University of Birmingham, Edgbaston, Birmingham B15 2TT, United

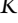


Kingdom;  [orcid.org/0000-0002-1043-7172](https://orcid.org/0000-0002-1043-7172);  
Email: [r.oreilly@bham.ac.uk](mailto:r.oreilly@bham.ac.uk)

## Authors

Irem Akar – School of Chemistry, University of Birmingham, Edgbaston, Birmingham B15 2TT, United Kingdom

Marcus C. Grocott – School of Chemistry, University of Birmingham, Edgbaston, Birmingham B15 2TT, United Kingdom

Amanda K. Pearce – School of Chemistry, University of Birmingham, Edgbaston, Birmingham B15 2TT, United Kingdom;  [orcid.org/0000-0003-3372-7380](https://orcid.org/0000-0003-3372-7380)

Complete contact information is available at:

<https://pubs.acs.org/10.1021/acsmacrolett.0c00645>

## Author Contributions

The manuscript was written through contributions of all authors.

## Notes

The authors declare no competing financial interest.

## ACKNOWLEDGMENTS

This work is supported by the Ministry of Turkish Education, EPSRC (EP/S00338X/1), ERC Consolidator Grant (No. 615142) and the University of Birmingham.

## REFERENCES

- (1) Gentekos, D. T.; Sifri, R. J.; Fors, B. P. Controlling polymer properties through the shape of the molecular-weight distribution. *Nat. Rev. Mater.* **2019**, *4*, 761–774.
- (2) Lynd, N. A.; Meuler, A. J.; Hillmyer, M. A. Polydispersity and block copolymer self-assembly. *Prog. Polym. Sci.* **2008**, *33*, 875–893.
- (3) Lodge, T. P. *Polymer Chemistry*; CRC Press, 2020.
- (4) Venkatram, S.; Kim, C.; Chandrasekaran, A.; Ramprasad, R. Critical Assessment of the Hildebrand and Hansen Solubility Parameters for Polymers. *J. Chem. Inf. Model.* **2019**, *59*, 4188–4194.
- (5) Foster, J. C.; Varlas, S.; Couturand, B.; Jones, J. R.; Keogh, R.; Mathers, R. T.; O'Reilly, R. K. Predicting Monomers for Use in Polymerization-Induced Self-Assembly. *Angew. Chem., Int. Ed.* **2018**, *57*, 15733–15737.
- (6) Varlas, S.; Foster, J. C.; Arkinstall, L. A.; Jones, J. R.; Keogh, R.; Mathers, R. T.; O'Reilly, R. K. Predicting Monomers for Use in Aqueous Ring-Opening Metathesis Polymerization-Induced Self-Assembly. *ACS Macro Lett.* **2019**, *8*, 466–472.
- (7) He, Y.; Eloi, J.-C.; Harniman, R. L.; Richardson, R. M.; Whittell, G. R.; Mathers, R. T.; Dove, A. P.; O'Reilly, R. K.; Manners, I. Uniform Biodegradable Fiber-Like Micelles and Block Comicelles via “Living” Crystallization-Driven Self-Assembly of Poly(l-lactide) Block Copolymers: The Importance of Reducing Unimer Self-Nucleation via Hydrogen Bond Disruption. *J. Am. Chem. Soc.* **2019**, *141*, 19088–19098.
- (8) Inam, M.; Cambridge, G.; Pitto-Barry, A.; Laker, Z. P. L.; Wilson, N. R.; Mathers, R. T.; Dove, A. P.; O'Reilly, R. K. 1D vs. 2D shape selectivity in the crystallization-driven self-assembly of polylactide block copolymers. *Chem. Sci.* **2017**, *8*, 4223–4230.
- (9) Akar, I.; Keogh, R.; Blackman, L. D.; Foster, J. C.; Mathers, R. T.; O'Reilly, R. K. Grafting Density Governs the Thermoresponsive Behavior of P(OEGMA-co-RMA) Statistical Copolymers. *ACS Macro Lett.* **2020**, *9*, 1149–1154.
- (10) Stubbs, C.; Murray, K. A.; Ishibe, T.; Mathers, R. T.; Gibson, M. I. Combinatorial Biomaterials Discovery Strategy to Identify New Macromolecular Cryoprotectants. *ACS Macro Lett.* **2020**, *9*, 290–294.
- (11) Southall, N. T.; Dill, K. A.; Haymet, A. D. J. A View of the Hydrophobic Effect. *J. Phys. Chem. B* **2002**, *106*, 521–533.
- (12) Chandler, D. Interfaces and the driving force of hydrophobic assembly. *Nature* **2005**, *437*, 640–647.
- (13) Sun, Q. The physical origin of hydrophobic effects. *Chem. Phys. Lett.* **2017**, *672*, 21–25.
- (14) Southall, N. T.; Dill, K. A. The Mechanism of Hydrophobic Solvation Depends on Solute Radius. *J. Phys. Chem. B* **2000**, *104*, 1326–1331.
- (15) Dharmaratne, N. U.; Jouaneh, T. M. M.; Kiesewetter, M. K.; Mathers, R. T. Quantitative Measurements of Polymer Hydrophobicity Based on Functional Group Identity and Oligomer Length. *Macromolecules* **2018**, *51*, 8461.
- (16) Gee, G. The interaction between rubber and liquids. III. The swelling of vulcanised rubber in various liquids. *Trans. Faraday Soc.* **1942**, *38*, 418–422.
- (17) Lipinski, C. A.; Lombardo, F.; Dominy, B. W.; Feeney, P. J. Experimental and computational approaches to estimate solubility and permeability in drug discovery and development settings. *Adv. Drug Delivery Rev.* **1997**, *23*, 3–25.
- (18) Bannan, C. C.; Calabró, G.; Kyu, D. Y.; Mobley, D. L. Calculating Partition Coefficients of Small Molecules in Octanol/Water and Cyclohexane/Water. *J. Chem. Theory Comput.* **2016**, *12*, 4015–4024.
- (19) Ghose, A. K.; Viswanadhan, V. N.; Wendoloski, J. J. Prediction of Hydrophobic (Lipophilic) Properties of Small Organic Molecules Using Fragmental Methods: An Analysis of ALOGP and CLOGP Methods. *J. Phys. Chem. A* **1998**, *102*, 3762–3772.
- (20) Lum, K.; Chandler, D.; Weeks, J. D. Hydrophobicity at Small and Large Length Scales. *J. Phys. Chem. B* **1999**, *103*, 4570–4577.
- (21) Li, I. T. S.; Walker, G. C. Single Polymer Studies of Hydrophobic Hydration. *Acc. Chem. Res.* **2012**, *45*, 2011–2021.
- (22) Ben-Amotz, D. Water-Mediated Hydrophobic Interactions. *Annu. Rev. Phys. Chem.* **2016**, *67*, 617–638.
- (23) Xi, E.; Patel, A. J. The hydrophobic effect, and fluctuations: The long and the short of it. *Proc. Natl. Acad. Sci. U. S. A.* **2016**, *113*, 4549–4551.
- (24) Wu, X.; Lu, W.; Streacker, L. M.; Ashbaugh, H. S.; Ben-Amotz, D. Temperature-Dependent Hydrophobic Crossover Length Scale and Water Tetrahedral Order. *J. Phys. Chem. Lett.* **2018**, *9*, 1012–1017.
- (25) Athawale, M. V.; Goel, G.; Ghosh, T.; Truskett, T. M.; Garde, S. Effects of lengthscales and attractions on the collapse of hydrophobic polymers in water. *Proc. Natl. Acad. Sci. U. S. A.* **2007**, *104*, 733–738.
- (26) Magenau, A. J. D.; Richards, J. A.; Pasquinelli, M. A.; Savin, D. A.; Mathers, R. T. Systematic Insights from Medicinal Chemistry To Discern the Nature of Polymer Hydrophobicity. *Macromolecules* **2015**, *48*, 7230–7236.
- (27) Yildirim, E.; Dakshinamoorthy, D.; Peretic, M. J.; Pasquinelli, M. A.; Mathers, R. T. Synthetic Design of Polyester Electrolytes Guided by Hydrophobicity Calculations. *Macromolecules* **2016**, *49*, 7868–7876.
- (28) Binkowski, T. A.; Naghibzadeh, S.; Liang, J. CASTp: Computed Atlas of Surface Topography of proteins. *Nucleic Acids Res.* **2003**, *31*, 3352–3355.
- (29) Connolly, M. L. Analytical molecular surface calculation. *J. Appl. Crystallogr.* **1983**, *16*, 548–558.
- (30) Bonn, R.; van Aartsen, J. J. Solubility of polymers in relation to surface tension and index of refraction. *Eur. Polym. J.* **1972**, *8*, 1055–1066.
- (31) van Oss, C. J.; Good, R. J. Surface Tension and the Solubility of Polymers and Biopolymers: The Role of Polar and Apolar Interfacial Free Energies. *J. Macromol. Sci., Chem.* **1989**, *26*, 1183–1203.
- (32) Koenhen, D. M.; Smolders, C. A. The determination of solubility parameters of solvents and polymers by means of correlations with other physical quantities. *J. Appl. Polym. Sci.* **1975**, *19*, 1163–1179.
- (33) Huggins, M. L. The Solubility of Nonelectrolytes. By Joel H. Hildebrand and Robert S. Scott. *J. Phys. Chem.* **1951**, *55*, 619–620.
- (34) Zhang, Q.; Weber, C.; Schubert, U. S.; Hoogenboom, R. Thermoresponsive polymers with lower critical solution temperature:

from fundamental aspects and measuring techniques to recommended turbidimetry conditions. *Mater. Horiz.* **2017**, *4*, 109–116.

(35) Wang, Y.; Nie, J.; Chang, B.; Sun, Y.; Yang, W. Poly-(vinylcaprolactam)-Based Biodegradable Multiresponsive Microgels for Drug Delivery. *Biomacromolecules* **2013**, *14*, 3034–3046.

(36) Hoogenboom, R. Temperature-Responsive Polymers: Properties, Synthesis, and Applications. In *Smart Polymers and their Applications*, 2nd ed.; Aguilar, M. R., San Román, J., Eds.; Woodhead Publishing, 2019; Chapter 2, pp 13–44.

(37) Roy, D.; Brooks, W. L. A.; Sumerlin, B. S. New directions in thermoresponsive polymers. *Chem. Soc. Rev.* **2013**, *42*, 7214–7243.

(38) Eggenhuisen, T. M.; Becer, C. R.; Fijten, M. W. M.; Eckardt, R.; Hoogenboom, R.; Schubert, U. S. Libraries of Statistical Hydroxypropyl Acrylate Containing Copolymers with LCST Properties Prepared by NMP. *Macromolecules* **2008**, *41*, 5132–5140.

(39) Djokpé, E.; Vogt, W. N-Isopropylacrylamide and N-Isopropylmethacrylamide: Cloud Points of Mixtures and Copolymers. *Macromol. Chem. Phys.* **2001**, *202*, 750–757.

(40) Becer, C. R.; Hahn, S.; Fijten, M. W. M.; Thijs, H. M. L.; Hoogenboom, R.; Schubert, U. S. Libraries of methacrylic acid and oligo(ethylene glycol) methacrylate copolymers with LCST behavior. *J. Polym. Sci., Part A: Polym. Chem.* **2008**, *46*, 7138–7147.

(41) Porsch, C.; Hansson, S.; Nordgren, N.; Malmström, E. Thermo-responsive cellulose-based architectures: tailoring LCST using poly(ethylene glycol) methacrylates. *Polym. Chem.* **2011**, *2*, 1114–1123.

(42) Yue, G.-l.; Cui, Q.-l.; Zhang, Y.-x.; Wang, E.-j.; Wu, F.-p. Thermo-responsive block copolymers based on linear-type poly(ethylene glycol): Tunable LCST within the physiological range. *Chin. J. Polym. Sci.* **2012**, *30*, 770–776.

(43) Luzon, M.; Boyer, C.; Peinado, C.; Corrales, T.; Whittaker, M.; Tao, L.; Davis, T. P. Water-soluble, thermoresponsive, hyperbranched copolymers based on PEG-methacrylates: Synthesis, characterization, and LCST behavior. *J. Polym. Sci., Part A: Polym. Chem.* **2010**, *48*, 2783–2792.

(44) Waggel, J.; Mathers, R. T. Post polymer modification of polyethylenimine with citrate esters: selectivity and hydrophobicity. *RSC Adv.* **2016**, *6*, 62884–62889.

(45) Mai, Y.; Eisenberg, A. Self-assembly of block copolymers. *Chem. Soc. Rev.* **2012**, *41*, 5969–5985.

(46) Brendel, J. C.; Schacher, F. H. Block Copolymer Self-Assembly in Solution—Quo Vadis? *Chem. - Asian J.* **2018**, *13*, 230–239.

(47) Sánchez-Iglesias, A.; Grzelczak, M.; Altantzis, T.; Goris, B.; Pérez-Juste, J.; Bals, S.; Van Tendeloo, G.; Donaldson, S. H.; Chmelka, B. F.; Israelachvili, J. N.; Liz-Marzán, L. M. Hydrophobic Interactions Modulate Self-Assembly of Nanoparticles. *ACS Nano* **2012**, *6*, 11059–11065.

(48) Cui, H.; Chen, Z.; Zhong, S.; Wooley, K. L.; Pochan, D. J. Block Copolymer Assembly via Kinetic Control. *Science* **2007**, *317*, 647–650.

(49) Yan, Y.; Huang, J.; Tang, B. Z. Kinetic trapping - a strategy for directing the self-assembly of unique functional nanostructures. *Chem. Commun.* **2016**, *52*, 11870–11884.

(50) Santos, J. L.; Herrera-Alonso, M. Kinetically Arrested Assemblies of Architecturally Distinct Block Copolymers. *Macromolecules* **2014**, *47*, 137–145.

(51) Zhang, Q.; Lin, J.; Wang, L.; Xu, Z. Theoretical modeling and simulations of self-assembly of copolymers in solution. *Prog. Polym. Sci.* **2017**, *75*, 1–30.

(52) Mastroianni, S. E.; Epps, T. H. Interfacial Manipulations: Controlling Nanoscale Assembly in Bulk, Thin Film, and Solution Block Copolymer Systems. *Langmuir* **2013**, *29*, 3864–3878.

(53) Blanz, A.; Madsen, J.; Battaglia, G.; Ryan, A. J.; Armes, S. P. Mechanistic Insights for Block Copolymer Morphologies: How Do Worms Form Vesicles? *J. Am. Chem. Soc.* **2011**, *133*, 16581–16587.

(54) Canning, S. L.; Smith, G. N.; Armes, S. P. A Critical Appraisal of RAFT-Mediated Polymerization-Induced Self-Assembly. *Macromolecules* **2016**, *49*, 1985–2001.

(55) Wang, X.; An, Z. New Insights into RAFT Dispersion Polymerization-Induced Self-Assembly: From Monomer Library, Morphological Control, and Stability to Driving Forces. *Macromol. Rapid Commun.* **2019**, *40*, 1800325.

(56) D'Agosto, F.; Rieger, J.; Lansalot, M. RAFT-Mediated Polymerization-Induced Self-Assembly. *Angew. Chem., Int. Ed.* **2020**, *59*, 8368–8392.

(57) Penfold, N. J. W.; Yeow, J.; Boyer, C.; Armes, S. P. Emerging Trends in Polymerization-Induced Self-Assembly. *ACS Macro Lett.* **2019**, *8*, 1029–1054.

(58) Varlas, S.; Foster, J. C.; O'Reilly, R. K. Ring-opening metathesis polymerization-induced self-assembly (ROMPISA). *Chem. Commun.* **2019**, *55*, 9066–9071.

(59) Degradation of Polymers. In *Comprehensive Chemical Kinetics*; Bamford, C. H., Tipper, C. F. H., Eds.; Elsevier, 2020; Vol. 14, pp 1–562.

(60) Chen, B.; van der Poll, D. G.; Jerger, K.; Floyd, W. C.; Frechet, J. M.; Szoka, F. C. Synthesis and properties of star-comb polymers and their doxorubicin conjugates. *Bioconjugate Chem.* **2011**, *22*, 617–24.

(61) Reis, R. L.; San Román, J. Understanding the enzymatic degradation of biodegradable polymers and strategies to control their degradation rate. In *Biodegradable Systems in Tissue Engineering and Regenerative Medicine*; Taylor and Francis, 2005; pp 177–201.

(62) Finnis, A.; Agarwal, S.; Gupta, R. Retarding hydrolytic degradation of polylactic acid: Effect of induced crystallinity and graphene addition. *J. Appl. Polym. Sci.* **2016**, *133*, na.

(63) Vey, E.; Rodger, C.; Meehan, L.; Booth, J.; Claybourn, M.; Miller, A. F.; Saiani, A. The impact of chemical composition on the degradation kinetics of poly(lactic-co-glycolic) acid copolymers cast films in phosphate buffer solution. *Polym. Degrad. Stab.* **2012**, *97*, 358–365.

(64) Aburto, J.; Alric, I.; Thiebaud, S.; Borredon, E.; Bikiaris, D.; Prinós, J.; Panayiotou, C. Synthesis, characterization, and biodegradability of fatty-acid esters of amylose and starch. *J. Appl. Polym. Sci.* **1999**, *74*, 1440–1451.

(65) Fields, R. D.; Rodriguez, F.; Finn, R. K. Microbial degradation of polyesters: Polycaprolactone degraded by *P. pullulans*. *J. Appl. Polym. Sci.* **1974**, *18*, 3571–3579.

(66) Makadia, H. K.; Siegel, S. J. Poly Lactic-co-Glycolic Acid (PLGA) as Biodegradable Controlled Drug Delivery Carrier. *Polymers* **2011**, *3*, 1377–1397.

(67) Mochizuki, M.; Hiram, M. Structural Effects on the Biodegradation of Aliphatic Polyesters. *Polym. Adv. Technol.* **1997**, *8*, 203–209.

(68) Min, K.; Cui, J. D.; Mathers, R. T. Ranking environmental degradation trends of plastic marine debris based on physical properties and molecular structure. *Nat. Commun.* **2020**, *11*, 727.